ing of the colored microspheres would have occurred. This would have resulted in few macrophages in the TBLN with 100 percent particle color homogeneity.

The probability that particles are translocated from the lung to the TBLN by macrophages has important implications. The movement of particles by this mechanism may be important in the dissemination of macrophage-resistant microorganisms that gain entry to the host by the respiratory tract. Inhaled toxic particles could be disseminated in a similar manner (*12*).

Immune responses induced to antigens deposited in the lungs may also be dependent on this mechanism of translocation. Potential allergens are constantly inhaled. If these allergens were translocated to the TBLN's, hypersensitivities could occur. Conversely, if an infectious microorganism were deposited in the lung, translocation of the antigens of the microorganism to the TBLN's would be necessary for the induction of an immune response against the microorganism. It has been shown that Langerhans' cells participate in immune responses by carrying antigen from the skin to the draining lymph nodes (*13*).

This study and that of Corry *et al.* (*7*) indicate that PAM's can migrate from the alveolus to the TBLN's. Our results also indicate that PAM's can transport particles to the TBLN's and therefore could determine the induction of lung immune responses by regulating antigen translocation to the TBLN's.

References and Notes

1. G. M. Green, *Arch. Intern. Med.* **131**, 109 (1973).
2. J. D. Brain, *ibid.* **126**, 477 (1970).
3. P. E. Morrow and C. L. Yuille, *Fundam. Appl. Toxicol.* **2**, 300 (1982).
4. D. E. Bice, D. L. Harris, B. A. Muggenburg, *Exp. Lung Res.* **1**, 33 (1980).
5. D. E. Bice, M. A. Degen, D. L. Harris, B. A. Muggenburg, *Am. Rev. Respir. Dis.* **126**, 635 (1982).
6. C. T. Schnizlein, D. E. Bice, C. E. Mitchell, F. F. Hahn, *Arch. Environ. Health* **37**, 201 (1982); D. E. Bice, J. L. Mauderly, R. K. Jones, R. O. McClellan, *Fundam. Appl. Toxicol.*, in press.
7. D. Corry, P. Kulkarni, M. F. Lipscomb, *Am. J. Pathol.* **115**, 321 (1984).
8. A. Johansson and P. Camner, *Toxicology* **15**, 157 (1980).
9. A. G. Harmsen, D. E. Bice, B. A. Muggenburg, *J. Leukocyte Biol.* **37**, 483 (1985).
10. M. B. Snipes, B. A. Muggenburg, D. E. Bice, *J. Toxicol. Environ. Health* **11**, 703 (1983).
11. J. D. Brain, S. P. Sorokin, J. J. Godleski, in *Respiratory Defense Mechanisms*, J. D. Brain, Ed. (Dekker, New York, 1977), vol. 2, pp. 849–889.
12. A. R. Brody, M. W. Roe, J. N. Evans, G. S. Davis, *Lab. Invest.* **47**, 533 (1982).
13. I. Silberg-Sinakin, G. J. Thorbecke, R. L. Baer, S. A. Rosenthal, V. Berezowsky, *Cell. Immunol.* **25**, 137 (1976).

14. Supported by Department of Energy contract DE-ACO4-76EV01013. We thank Mike Jarpe for technical assistance and Dr. Robert Jones and the other staff members at the Inhalation Toxicology Research Institute who made helpful suggestions during the preparation of this report.

31 May 1985; accepted 3 October 1985

Myofibrils Bear Most of the Resting Tension in Frog Skeletal Muscle

Abstract. *The tension that develops when relaxed muscles are stretched is the resting (or passive) tension. It has recently been shown that the resting tension of intact skeletal muscle fibers is equivalent to that of mechanically skinned skeletal muscle fibers. Laser diffraction measurements of sarcomere length have now been used to show that the exponential relation between resting tension and sarcomere length for whole frog semitendinosus muscle is similar to that of single fibers. Slack sarcomere lengths and the rates of stress relaxation in these muscles were similar to those in skinned fibers, and sarcomere length remained unchanged during stress relaxation, as in skinned fibers. Thus, in intact semitendinosus muscle of the frog up to a sarcomere length of about 3.8 micrometers, resting tension arises, not in the connective tissue as is commonly thought, but in the elastic resistance of the myofibrils.*

ALAN MAGID
DOUGLAS J. LAW
Department of Anatomy, Duke University Medical Center, Durham, North Carolina 27710

A simple form of muscular force is the "passive" tension that results when resting muscles are stretched. The sum of the passive and active tensions is the total force acting to shorten a muscle. Passive tension is commonly attributed to elastic forces in the connective tissue and not to myofibrillar elasticity (*1–3*). This early view contrasts sharply with the more recent demonstration that the passive tension of single fibers is borne largely by the myofibrils, with a small contribution at extreme length from the collagen fibrils in the sarcolemma (*4–7*). To what extent might this also be true for whole muscles?

To answer this question, we have measured the variation of passive tension with sarcomere length (S) in intact frog semitendinosus muscles. Muscles (*8*) were stretched in increments, and the tension was permitted to relax until it became steady or nearly so, that is, until it exhibited changes of less than 1 percent per minute (*9*). For measurements of S, a narrow beam of coherent light from a He-Ne laser could be directed at any point on the muscle. The diffraction pattern from the chosen region fell upon a ground-glass screen 300 mm away. S was calculated from the positions of the diffraction fringes, marked directly on the screen or photographed with a 35-mm camera (*10*).

When a resting muscle was quickly stretched, tension rose immediately and then began to decay as soon as stretching stopped (Fig. 1A). S remained constant (changed less than ±1 percent) during stress relaxation (Fig. 1B). The extent of stress relaxation increased with each step in length. These force responses showed no sign of the delayed rise often seen when activated muscles are stretched (stretch activation), nor did they show any sign of the short-range elastic component attributed by Hill (*11*) to a few weakly attached cross-bridges. These findings indicate that the forces studied here are purely passive. One indication that this force is viscoelastic and not simply viscous is that muscles that were held stretched overnight remained taut.

The length-tension curves in four resting muscles (Fig. 2A) represent the range of variation encountered in this study. Tension increased exponentially with S in all cases. The curves in Fig. 2A are calculated from the expression (*12*)

$$\sigma = \frac{E_0}{\alpha}\,(e^{\alpha\epsilon_s} - 1) \qquad (1)$$

where σ is stress (force per cross-sectional area), E_0 is the initial elastic modulus, α is an empirical constant, and ϵ_s is

Table 1. Values of α and E_0 for the length-tension equation for resting muscles, Eq. 1. Tabulated are means ± standard error of the mean (SEM). Data for intact fibers are from Rapaport (*5*); skinned fiber data are from Magid (*7*). The value of α for whole muscle does not differ significantly from that for intact fibers or skinned fibers ($P = 0.287$, analysis of variance, rank 2 affine hypothesis). The differences among E_0 values are significant ($P < 0.001$).

Preparation	Number of samples	Exponent α	Initial elastic modulus, E_0 ($\times 10^3$ N/m^2)
Whole muscles	11	4.28 ± 0.19	2.6 ± 0.25
Intact single fibers	10	4.04*	9.8*
Skinned single fibers	12	4.13 ± 0.10	5.4 ± 0.75

*No SEM's are reported because the values come from a single analysis of pooled data.

sarcomere strain, $S/S_0 - 1$; we used values of α and E_0 obtained from a plot of the natural logarithm of stress versus strain (Fig. 2B). The curves for muscles 2 and 3 have similar shapes, but the values of α and E_0 differ; as expected from Eq. 1, both α and E_0 interact to control the "stiffness" of the muscle. Average values of α and E_0 for whole muscles are shown in Table 1, together with the same parameters for intact and mechanically skinned single fibers from semitendinosus muscles.

Values of α for whole muscles and single fibers are not significantly different (Table 1), an indication that the curvature of the length-tension relation is the same for all. E_0 for whole muscle appears smaller than that for single fibers, but this must reflect systematic differences in the methods for estimating cross-sectional area in the different studies. Whole muscles cannot bear less tension than their component fibers.

Other similarities emerge when whole muscle and single fibers are compared. S_0 in whole muscle (2.14 ± 0.02 μm) is very close to the value observed in skinned semitendinosus fibers [2.16 ± 0.04 μm (*7*)]. Thus the plasma membrane, connective tissue, and resting calcium levels do not substantially affect equilibrium rest length; rather, rest length is established by forces intrinsic to the resting sarcomere. As with skinned fibers, S remains unchanged during stress relaxation in whole muscle. This finding and the simple kinetics (Fig. 1) indicate that stress relaxation proceeds uniformly in each sarcomere. Further, the rates of stress relaxation in whole muscle and their dependence on stress are similar to those in skinned fibers (*13*).

These findings are at odds with the widely accepted idea that the connective tissue is responsible for the resting tension. Aside from its appeal to common sense, support for this view comes largely from two early studies (*1, 2*). Banus and Zetlin (*1*) reported that resting tension in frog gastrocnemius muscles was unaffected after the muscle fibers were removed. This claim is difficult to evaluate because their procedure was not described and no anatomical data were given. Ramsey and Street (*2*) reported that the resting tension in sarcolemmal tubes was the same as that in single fibers, but this conclusion was later retracted (*14*).

What role then does the connective tissue play? We believe that its contribution to resting tension in whole semitendinosus muscle becomes important only at sarcomere lengths greater than ~3.8 μm. Four observations support this view. (i) Rapaport showed this for single intact fibers (*4, 5*) [other findings are qualitatively consistent with this view (*15*)]. (ii) Passive tension in mechanically skinned fibers drops substantially below exponential increase at about this length (*6, 7*), whereas in whole muscles it does not (Fig. 2A). (iii) Schmalbruch (*16*) reported that the collagen fibrils of the sarcolemma were initially slack but became aligned with the fiber axis at the length where resting tension increased sharply. (iv) Mechanically skinned rat cardiac myocytes, though showing appreciable resting tension, can be stretched farther than intact cells (*17*).

On the basis of these considerations we conclude that, over the range of sarcomere lengths involved in natural movement (*18*), the passive resistance to stretching arises largely in the myofibrils. What component of the sarcomere embodies this resting elasticity? In insect flight muscle, filamentous connections between thick filaments and Z lines serve this function (*19*). A similar arrangement has been proposed for vertebrate striated muscles (*6, 7*).

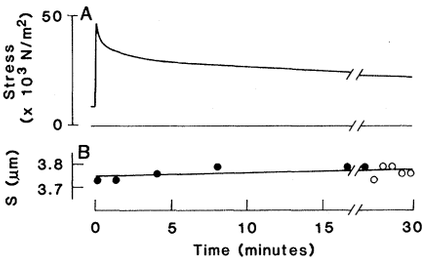

Fig. 1. (A) Force transient from a resting muscle quickly stretched from S = 3.3 to 3.7 μm. The time course of stress relaxation was analyzed in each of the records from this muscle. Two exponential processes were detected; both slowed with increasing strain. The first process was too fast to characterize accurately from our records. The second process was much slower (and larger), having time constants that varied linearly with stress from 50 seconds at S = 2.7 μm to 1180 seconds at S = 4.2 μm. (B) Sarcomere length (S) measured at a fixed point during tension decay (closed circles); S remained virtually unchanged during stress relaxation. Values of S observed at successive points along the muscle (open circles). Since the two types of length measurements barely differ, observations made at a single point (the usual scheme in this study) are representative.

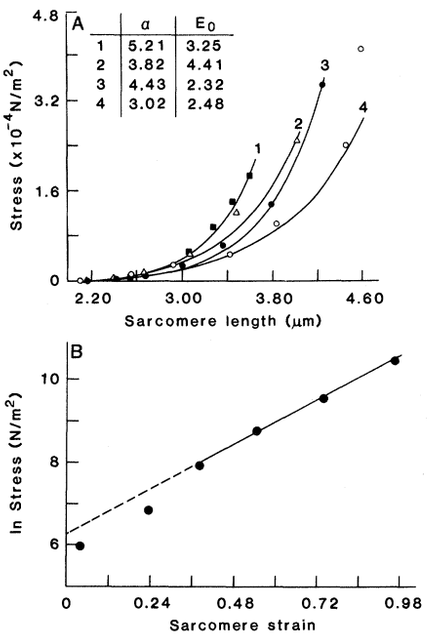

Fig. 2. (A) Length-tension relation in four resting muscles. Tabulated are the values used in Eq. 1 to draw the solid line. (B) Stress-strain relation for muscle 3. After taking logarithms, Eq. 1 becomes (when $e^{\alpha\epsilon} >> 1$)

$$\ln \sigma \approx \alpha\epsilon_s + \ln E_0/\alpha \quad (2)$$

Data from muscle 3 are plotted here according to Eq. 2. The solid line is a linear regression to the values above a strain of 0.3. The slope is α; E_0 is obtained from the y-intercept, ln E_0/α.

References and Notes

1. M. G. Banus and A. M. Zetlin, *J. Cell. Comp. Physiol.* **12**, 403 (1938).
2. R. W. Ramsey and S. F. Street, *ibid.* **15**, 11 (1940).
3. A. V. Hill, *Nature (London)* **166**, 415 (1950).
4. S. I. Rapaport, *J. Gen. Physiol.* **59**, 559 (1972).
5. _____, *Biophys. J.* **13**, 14 (1973).
6. A. Magid, *ibid.* **41**, 35a (1983); A. D. Magid *et al.*, in *Contractile Mechanisms in Muscle*, G. H. Pollack and H. Sugi, Eds. (Plenum, New York, 1984), pp. 307–322.
7. A. Magid, in preparation.
8. Frogs (*Rana pipiens*) averaged 7.0 cm (range, 6.3 to 8.5 cm) from nose to vent. Semitendinosus muscles averaged 20.3 mm in length (range, 17 to 24 mm). Cross-sectional area (A) was estimated from the width (w) and thickness (t), measured on a microscope, based on an elliptical profile [$A = \pi/4(wt)$]. Confirmation of this assumption was obtained from micrographs of muscle cross sections.
9. After carefully cutting away the ventral head of the semitendinosus muscle, we tied delicate stainless steel hooks to the tendons of the dorsal head, close to the muscle belly. Muscles were soaked for several hours in normal or calcium-free Ringer solution and then mounted in the experimental chamber. Ringer solution had the following composition (micromolar): NaCl, 115; KCl, 2.5; $CaCl_2$, 1.8; $MgCl_2$, 1.0; sodium phosphate, 3; pH, 7.2. Calcium-free Ringer solution had the composition (micromolar): NaCl, 100; KCl, 2.5; $MgCl_2$, 4; Na_2EGTA, 5; MOPS [2-(*N*-morpholino)propane sulfonic acid], 3; pH, 7.2. No difference was detected between muscles studied in either saline. Muscles were mounted vertically, with one hook fixed near the bottom of the chamber and the other attached, through a rigid link, to a force transducer (Grass FT 03C). Length changes were produced with a rack-and-pinion device to which the transducer was attached. We determined slack sarcomere length (S_0) by releasing the slightly taut muscle until no drop in tension was detected. The limit of detection was about 1 dyne. Experiments were done at room temperature (20° to 22°C).
10. S was calculated from the plane grating equation, $S = \lambda/\sin\theta$, where λ is the wavelength (0.633 μm) and θ is the angle between the zero- and first-order diffracted rays.
11. D. K. Hill, *J. Physiol. (London)* **199**, 637 (1968).
12. O. Sten-Knudsen, *Acta Physiol. Scand. Suppl.* **28**, 104 (1953).
13. A. Magid, unpublished data.
14. S. F. Street, *J. Cell. Physiol.* **114**, 346 (1983).
15. X. Aubert, M. L. Roquet, J. Van der Elst, *Arch. Int. Physiol.* **59**, 239 (1951); F. Buchtal, E. Kaiser, P. Rosenfalck, *Dan. Biol. Medd.* **21**, 1 (1951); C. Casella, *Acta Physiol. Scand.* **21**, 380 (1951); R. Natori, *Jikeikai Med. J.* **1**, 119 (1954);

R. J. Podolsky, *J. Physiol. (London)* **170**, 110 (1964).
16. H. Schmalbruch, *Cell Tissue Res.* **150**, 377 (1974).
17. A. Fabiato and F. Fabiato, *J. Gen. Physiol.* **72**, 667 (1978).
18. To estimate the range of S values during movement, all muscles except the semitendinosus were removed from frog hindlimbs and the legs were then set in various positions approximating those seen in living animals. The preparation was supported in a transparent bath and illuminated from above with a laser. When the frog was "sitting," the muscles were slack ($S \sim 2.1$ μm); with the leg pointing fully forward, S was ~3.0 μm; with extreme flexing at the hip and knee, the muscle was brought to filament non-overlaps ($S \sim 4.2$ μm) (A. Magid and M. Carvell, unpublished data).
19. D. C. S. White, thesis, Oxford University (1967); *J. Physiol. (London)* **343**, 31 (1983).
20. We are grateful to M. K. Reedy for providing laboratory facilities. We thank M. K. Reedy, B. McDonald, H. Erickson, W. Longley, T. McIntosh, and K. Smith for valuable suggestions regarding the text. We thank R. Wolpert, who provided help with the statistical analysis. An account of this work was presented at the 1985 annual meeting of the Biophysical Society. Research supported by grants from the NIH (AM27763) and the North Carolina United Way.

25 March 1985; accepted 1 August 1985

The Human Gene Encoding GM-CSF Is at 5q21-q32, the Chromosome Region Deleted in the 5q⁻ Anomaly

Abstract. *Human granulocyte-macrophage colony-stimulating factor (GM-CSF) is a 22,000-dalton glycoprotein that stimulates the growth of myeloid progenitor cells and acts directly on mature neutrophils. A full-length complementary DNA clone encoding human GM-CSF was used as a probe to screen a human genomic library and isolate the gene encoding human GM-CSF. The human GM-CSF gene is approximately 2.5 kilobase pairs in length with at least three intervening sequences. The GM-CSF gene was localized by somatic cell hybrid analysis and in situ hybridization to human chromosome region 5q21-5q32, which is involved in interstitial deletions in the 5q⁻ syndrome and acute myelogenous leukemia. An established, human promyelocytic leukemia cell line, HL60, contains a rearranged, partially deleted GM-CSF allele and a candidate 5q⁻ marker chromosome, indicating that the truncated GM-CSF allele may reside at the rejoining point for the interstitial deletion on the HL60 marker chromosome.*

KAY HUEBNER
MASAHARU ISOBE
CARLO M. CROCE
The Wistar Institute, Philadelphia, Pennsylvania 19104
DAVID W. GOLDE
SUSAN E. KAUFMAN
JUDITH C. GASSON
Division of Hematology-Oncology, School of Medicine, University of California, Los Angeles 90024

Colony-stimulating factors (CSF's), proteins required for proliferation and differentiation of hematopoietic progenitor cells, are produced by a variety of human and murine cell types (*1*), including established cell lines (*2*). We previously described the purification of a 22,000-dalton glycoprotein with granulocyte-macrophage colony-stimulating activity (GM-CSF) from medium conditioned by the HTLV-II–infected human T-lymphoblast cell line Mo (*3*). Purified biosynthetic (recombinant) GM-CSF has all of the biological activities attributed to the protein purified from Mo-conditioned medium (*3, 4*). Differential staining of cells in bone marrow–derived colonies that had been stimulated by this GM-CSF demonstrated that the mediator induces growth of granulocyte, granulocyte-macrophage, macrophage, and eosinophil colonies (*5*). In addition, purified GM-CSF stimulates colony formation by the HL60 and KG-1 leukemic cell lines and is a weak inducer of differentiation in HL60 cells (*5*). Neutrophil migration in agarose is inhibited by purified natural and biosynthetic GM-CSF (*3*), and neutrophil oxidative metabolism is potentiated by GM-CSF (*6, 7*), suggesting an important role for this mediator in both the production and function of granulocytes for host defense.

High molecular weight DNA was prepared from the Mo (*8*) and J-WM-III (*9*) HTLV-II–infected T-lymphoblast cell lines, the K562 (*10*) human erythroleukemia cell line, and the WIL-2 human B-cell line and analysed (*11*) for hybridization to a GM-CSF–complementary DNA (cDNA) clone (*4*). Single fragments of approximately 8.0 kilobases (kb) and 5.2 kb were seen after digestion with Bam HI and Hind III, respectively. Fragments of 3.8 and 2.7 kb were detected after digestion with Bgl II. No differences in restriction fragment lengths were seen among DNA's from these cell lines, nor when Mo and human liver high molecular weight DNA's were compared (*4*). As digestion with Bgl II yielded two fragments that hybridize to the cDNA clone, which itself has no internal Bgl II sites, the GM-CSF gene contains at least one intron.

The GM-CSF gene was isolated from normal DNA in order to determine its structural organization. A recombinant phage library (*12*) (prepared from Charon 4a and fetal liver DNA) was screened with the GM-CSF cDNA clone as a probe. Two genomic GM-CSF clones were obtained from approximately 750,000 recombinant phage. The clones each contained the Bam HI, Hind III, and both Bgl II restriction fragments detected by DNA hybridization analysis (Fig. 1, CSF-2; the map was the same for both clones). Further comparative restriction enzyme mapping of the genomic and cDNA clones revealed the existence of at least three introns in the human GM-CSF gene (Fig. 1). The total length of the gene is approximately 2.5 kb.

A panel of 25 mouse-human hybrids (*13*), retaining defined subsets of human chromosomes, was analyzed for the presence of the GM-CSF gene by hybridization of their DNA with the genomic clone of the 5.2-kb Hind III fragment as a probe (pCH5.2, Fig. 1). After hybridization of pCH5.2 plasmid DNA to Hind III–digested DNA from a normal donor, a single band of approximately 5.2 kilobase pairs (kbp) was seen, while mouse

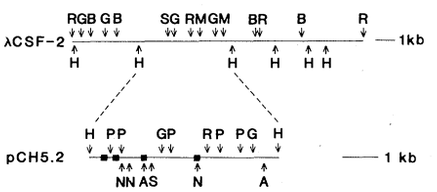

Fig. 1. Genomic map of the human GM-CSF gene. A bacteriophage λ recombinant library (*12*) was propagated on DP50 supf bacteria with ~25,000 recombinant phage per 100-cm plate. The library was screened by plaque hybridization with the full-length gel-purified GM-CSF cDNA clone that had been labeled with ^{32}P by nick translation. Restriction maps were obtained by digesting DNA with various restriction enzymes, fractionating the digests on agarose gels, transferring the DNA to nitrocellulose filters, and hybridizing the filters with the ^{32}P-labeled GM-CSF cDNA insert. The 5.2-kb Hind III fragment of the CSF-2 that hybridized to the GM-CSF cDNA clone was subcloned into the Hind III site of pBR322 (pCH 5.2). In the construction of restriction maps for the subclone, the hybridization probe consisted of two smaller fragments of the GM-CSF cDNA clone that were prepared with Apa I and Eco RI, gel purified, nick translated, and hybridized individually to restriction endonuclease–digested pCH5.2 DNA. The fragments generated by digestion of the GM-CSF cDNA insert with Apa I represent nucleotides 1 to 288 (5′) and 289 to 780 (3′). The sites of cleavage for Eco RI (R), Sal I (S), Sma I (M), Hind III (H), Bgl II (G), Bam HI (B), Apa I (A), Nco I (N), and Pvu II (P) are shown.